

# The influence of the ethanol/water molar ratio in the precursor solution on morphology and photocatalytic activity of pyrolytic ZnO films

María Quintana<sup>(1)</sup>; Juan Rodríguez<sup>(2,1)</sup> [jrodriguez@ipen.gob.pe](mailto:jrodriguez@ipen.gob.pe); José Solís<sup>(2,1)</sup> [jsolis@ipen.gob.pe](mailto:jsolis@ipen.gob.pe);  
Walter Estrada<sup>(2,1)</sup> [westrada@ipen.gob.pe](mailto:westrada@ipen.gob.pe)

(1) *Universidad Nacional de Ingeniería, Facultad de Ciencias, Av. Tupac Amaru 210, Lima 25, Perú*

(2) *Instituto Peruano de Energía Nuclear (IPEN), Av. Canadá 1470, Lima 41, Perú*

## Abstract

Zinc oxide films were fabricated by a home made spray pyrolysis system equipped with an optical set-up ensuring the in-situ control of the film growth. 0.1 M of zinc acetate diluted in a mixture of ethanol and water was used as the precursor solution. The ethanol/water molar ratio,  $\Gamma$ , in the precursor solution was varied from 0 to 0.92. The deposition temperature and the pH of the precursor solution were kept at 350 °C and 4.5, respectively. X-ray diffraction patterns revealed that films were zincite-like with a grain size depending of the ethanol/water molar ratio in the precursor solution. The interference pattern obtained during film deposition was used to monitor the film roughness; it was found that this is related with those results of surfaces and optical analysis obtained by scanning electron microscopy (SEM) and spectrophotometric measurements, respectively. The morphology of the ZnO films obtained from  $\Gamma$  equal to either 0 or 0.92 are dense with agglomerates uniformly distributed, whereas the films obtained from  $\Gamma$  equal to 0.03 or 0.06 are very rough with irregular agglomerates. The films obtained from  $\Gamma$  equal to 0.12, 0.18 and 0.31 are rough. Photo-electrocatalytic results indicated that there is a correlation of the partial molar volume of ethanol respect to water in the spraying solution with the photocatalytic efficiency of the ZnO films. We found that the maximum photodegradation of methyl orange in the solution occurs using ZnO films obtained with  $\Gamma$  equal to 0.12.

## 1. Introduction

Rough thin films are of much interest for applications in photo-electrocatalysis, gas sensors, solar photoelectrochemical cells, etc., due to the large interface between the solid and the fluid surrounded it. Photocatalytic degradation of organic compounds has been proposed as viable alternative for the decontamination of either waste water or drinking water for human use (1). Titanium oxide is by far the most studied material for those applications (2). However, zinc oxide can be used as well for this purpose (3). Thin film morphology depends on the deposition technique and different techniques have been reported for preparing ZnO films: sol-gel (4), reactive evaporation (5), sputtering (6), chemical bath (7), spray pyrolysis (8-11), etc. Among these techniques, spray pyrolysis is one of the most simple and inexpensive technique, and the film morphology can be easily monitored controlling the precursor and deposition conditions. Transparent ZnO-based films have been obtained by pyrolytic decomposition of zinc acetate diluted in ethanol (12), in de-ionized water (13, 14) or a

mixture (3:1 vol.) of ethanol and de-ionized water (15). Recently, we have reported the influence in the film roughness of the pH in the precursor solution (zinc acetate diluted in water), and the degradation of methyl orange has been more efficient with rough films (13). In this work we report the influence in the ZnO film morphology of zinc acetate dilution at different mixtures of water and ethanol. The film growth was monitored by in situ laser reflectometry, and the photo-electrocatalytic degradation of methyl orange in aqueous solution using ZnO thin films was studied. The efficiency of methyl orange degradation is shown to be related to the roughness of the film.

## 2. Materials and Methods

### 2.1 Film preparation and in-situ film growth monitoring.

Zinc oxide films were deposited using a home made spray pyrolysis system described elsewhere (14). A medical nebulizer was used as the atomizer. The process starts from the aerosol of the precursor solution produced in the nebulizer, which is sprayed onto a hot substrate where the film is going to grow. A 0.1 M starting

solution of extra pure hydrated zinc acetate (Riedel-de-Häen, Seelze, Germany) in a mixture of deionized water and ethanol was used in all experiments. Some drops of acetic acid (Mallinckrodt Laboratory Chemicals, Phillipsburg, USA) were added to obtain a total dissociation of the zinc acetate. Different amounts of ethanol (Merck, Darmstadt, Germany) were in the starting solution, so that the molar ethanol/water ratio,  $\Gamma$ , in the zinc acetate solution was varied from 0 to 0.92. Acetic acid drops were added in order to adjust the pH of the solution at 4.5. Compressed air was used as a gas carrier with a flux and air pressure kept at 15 l/min and  $1.7 \times 10^5$  Pa, respectively. The solutions were sprayed onto the substrate at 350 °C. A laser reflectometry system for in-situ monitoring the film growth during deposition was set up. This is described elsewhere (unpublished work).

ZnO films were deposited onto 2-mm-thick Libbey Owens Ford glass substrates precoated with a layer of transparent and conducting  $\text{SnO}_2:\text{F}$  having a resistance/square of 8  $\Omega$ . In order to have films with the same thickness, the spraying was stopped when the in situ laser reflectance signal as a function of deposition time showed three interference peaks ( $\approx 650$  nm thick). Film thickness measured by a Tencor alpha step profilometer, gave an average value of  $600 \pm 40$  nm. The in situ laser reflectance patterns for ZnO films prepared from different molar ethanol/water ratio in the precursor solution are shown in Fig. 1. In all films, oscillations and progressive attenuation of the reflectivity were observed as the film grows. The maxima and minima in the reflectivity define an envelope within the reflectivity oscillates, which is associated to the film roughness. The degree of roughness in the film is related how fast the amplitude of the envelope decrease; for an ideal specular film the amplitude of the envelope does not decrease. We observed that the films become roughest at  $\Gamma \approx 0.06$ ; the film roughness for those prepared at  $\Gamma$  lower or higher than 0.06 decrease progressively. The films recover their optical specularity, characterized by a well defined interference fringes, when are prepared at either  $\Gamma = 0$  or  $\Gamma = 0.92$ .

**2.2 Optical and structure characterization.** Spectral specular transmittance ( $T_s$ ) and reflectance ( $R_s$ ), and spectral diffuse transmittance ( $T_d$ ) and reflectance ( $R_d$ ) for

ZnO films were recorded in the  $300 < \lambda < 2500$  nm wavelength range using a Perkin Elmer lambda 9 double beam spectrophotometer equipped with an integrating sphere. The crystal structures of the obtained films were characterized by X-ray diffraction (XRD) using a Phillips X Pert diffractometer operating with  $\text{CuK}_\alpha$  radiation. Surface morphologies were studied with a scanning electron microscopy (SEM) using a Philips 300 instrument operated at 20 kV.

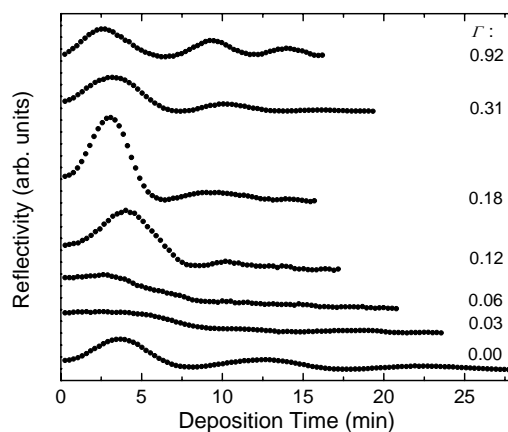


**Figure 1.** In-situ normal reflectance of a 632.8 nm laser as a function of time for pyrolytic ZnO films obtained using a precursor solution with the shown ethanol/water molar ratio,  $\Gamma$ .

**2.3 Photo-electrocatalytic degradation of methyl orange.** The photo-electrocatalytic degradation of a methyl orange (Merck, Darmstadt, Germany) water solution using the as-deposited ZnO films was studied using a photoreactor described elsewhere (16). It consists of a Teflon cylindrical container where a sample with ZnO film facing to the interior was mounted in the open end that can be irradiated by ultraviolet (UV) light and filled with  $35 \times 10^{-5}$  M of methyl orange aqueous solution. Two parallel quartz windows are aligned perpendicularly to the cylinder axis in order to allow spectrophotometric transmittance measurements of the solution. A three-electrode arrangement was used in the experiments. It includes a Pt foil as counter electrode, ZnO coating as the working electrode and an Ag/AgCl electrode as the reference electrode. UV irradiation was accomplished with a Phillips Hg 250 W lamp mounted 15 cm in front of the sample. In order to avoid thermal effects, a water filter was used between the lamp and the photoreactor. The intensity of the UV-A spectrum (310 to 400 nm) - measured with an UDT 300 radiometer - was 3 mW. The

photoreactor was positioned in the sample compartment of the RS 325 Optometrics spectrophotometer and a mechanical chopper system was used to avoid the UV irradiation during spectrophotometer recordings. A Wenking POS 73 potentiostat interfaced to a computer was used for electrochemical measurements. An applied bias potential of 0.7 V to the working electrode was used to avoid electron-hole recombination in the irradiated samples; this effect may otherwise be significant, mainly due to traps and surface states. In order to diminish the influence of free oxygen, a well-known electron scavenger of nitrogen bubbles was used continuously into the sample compartment so that the solution was kept uniformly mixed.

### 3. Results

**3.1 Optical characterization.** Figure 2 shows the spectral specular transmittance ( $T_s$ ) for ZnO films deposited onto glass with the shown  $\Gamma$  values of the precursor solution. A noticeable change in the specular transmittance is observed in the films if  $\Gamma$  varies. It is observed that the overall spectral specular transmittance decreases when  $\Gamma$  decreases from 0.92 to 0.06, and increases for  $\Gamma$  values lower than 0.06. The films obtained with  $\Gamma$  equal either to 0.92 or 0.00 are transparent films. The ZnO films obtained at  $\Gamma$  equal to 0.03, 0.06 and 0.12 did not show any interference pattern. In those films the rough surface scatters the light and destroys the interference effects, also they have a milky appearance, and are highly diffusive films.

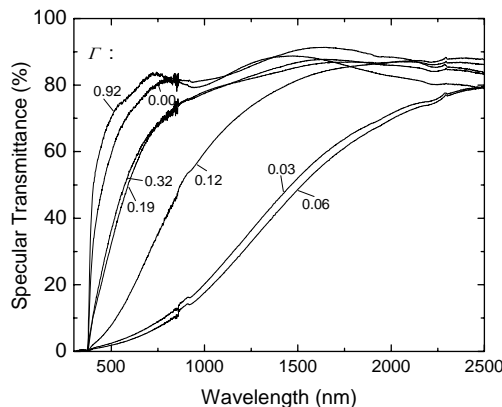


**Figure 2.** Spectral measured specular transmittance for pyrolytic ZnO films deposited onto glass at 350 °C using a precursor solution with the shown ethanol/water molar ratio,  $\Gamma$ .

$T_s$ ,  $T_d$ ,  $R_s$  and  $R_d$  measured at 550 nm as a function of  $\Gamma$  in the precursor solution is shown in Fig. 3. From this graph is clearly observed that the  $T_s$  and  $R_s$  follow the same behavior. Minimum values are obtained at  $\Gamma = 0.06$ ; whereas the  $T_d$  and  $R_d$  follows a reverse trend, i.e.  $T_d$  and  $R_d$  reach a maximum at  $\Gamma = 0.06$ . The  $T_d$  and  $R_d$  are related with the roughness of the film.

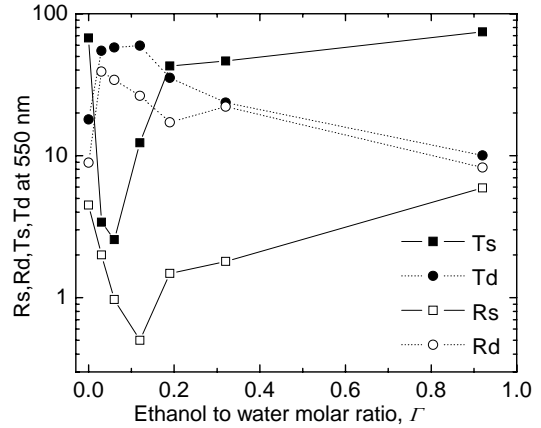


**Figure 3.** Specular transmittance  $T_s$ , diffuse transmittance  $T_d$ , specular near normal reflectance  $R_s$  and diffuse near normal reflectance  $R_d$  measured at 550 nm for pyrolytic zinc oxide films as a function of the ethanol/water molar ratio,  $\Gamma$ , in the precursor solution.

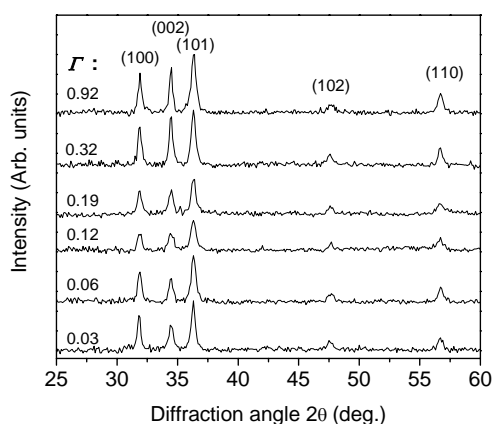
**3.2 Structure characterization.** Figure 4 displays XRD data for zinc oxide films deposited at six different  $\Gamma$ 's in the precursor solution on to glass substrates. It is evident that the films regardless of  $\Gamma$  consist of a zincite like structure, diffraction peaks at (100), (002), (101), (102) and (110) directions are observed. The mean grain size  $D$  was estimated from Scherrer's formula, i.e.,

$$D = \frac{0.9\lambda_x}{\beta \cos\theta}, \quad (1)$$

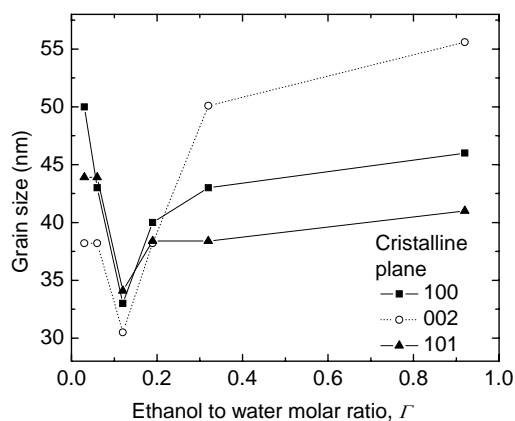
where  $\lambda_x = 1.54 \text{ \AA}$  is the X-ray wavelength of the  $\text{CuK}\alpha$  radiation,  $2\theta$  is the diffraction angle, and  $\beta$  is the full width at half maximum of diffraction peak. Applying Scherrer's formula to (100), (002) and (101) peaks for ZnO films, the grain size was found that depends on the  $\Gamma$  value used in the precursor solution (see Fig. 5). Regardless the peaks used to derive the grain size of the ZnO films, it has a minimum around 33 nm at  $\Gamma = 0.12$ .

Figure 6 displays the morphology of zinc oxide films obtained at different  $\Gamma$  values in the precursor solution, onto a transparent- $\text{SnO}_2$ : F-precoated glass substrate. The

morphology of the ZnO films obtained with  $\Gamma$  equal to 0 and 0.92 are dense with agglomerates uniformly distributed, whereas the films obtained with  $\Gamma$  equal to 0.03 and 0.06 are very rough with irregular agglomerates. ZnO films obtained with  $\Gamma$  equal to 0.12, 0.18 and 0.32 are less dense than the films obtained with  $\Gamma$  equal to 0 and 0.92. This is in agreement with the results obtained by optical characterization.



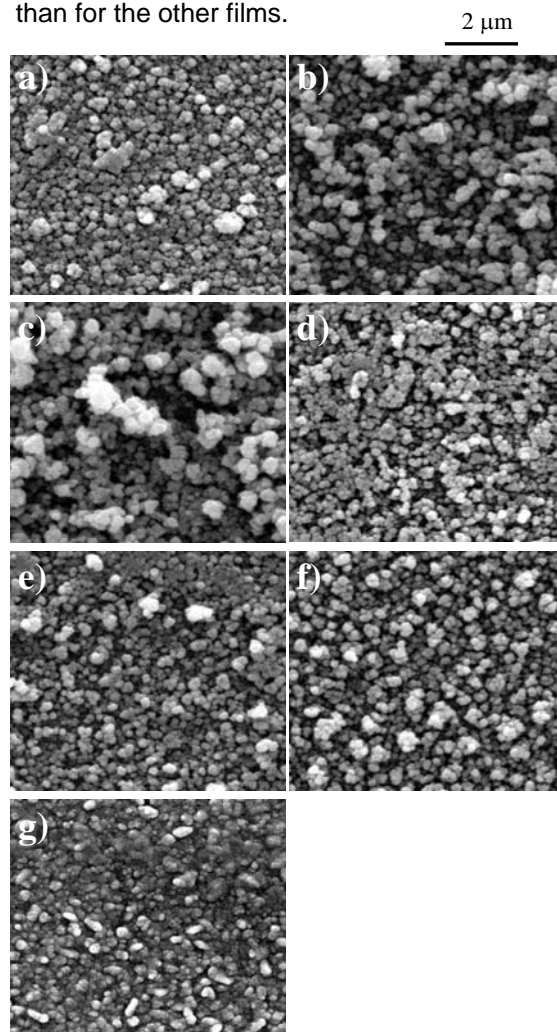
**Figure 4.** X ray diffractograms for pyrolytic zinc oxide films obtained using a precursor solution with the shown ethanol/water molar ratio,  $\Gamma$ .



**Figure 5.** Grain size of pyrolytic ZnO films as a function of the ethanol/water molar ratio,  $\Gamma$ , in the precursor solution.

**3.3 Photo-electrocatalytic degradation of methyl orange.** Films prepared at lower partial molar volume of ethanol respect to water in the spraying solution ( $\Gamma=0.06$  and  $\Gamma=0.03$ ) shown to be mechanically instable in water, so photo-electrocatalytic degradation studies for those films were not performed. Fig. 7 shows measured data on photocurrent for ZnO films obtained with  $\Gamma$  equal to 0.12, 0.32 and 0.92 in the precursor solution as a function of irradiation time. The breaks in the photocurrent were caused by the chopper,

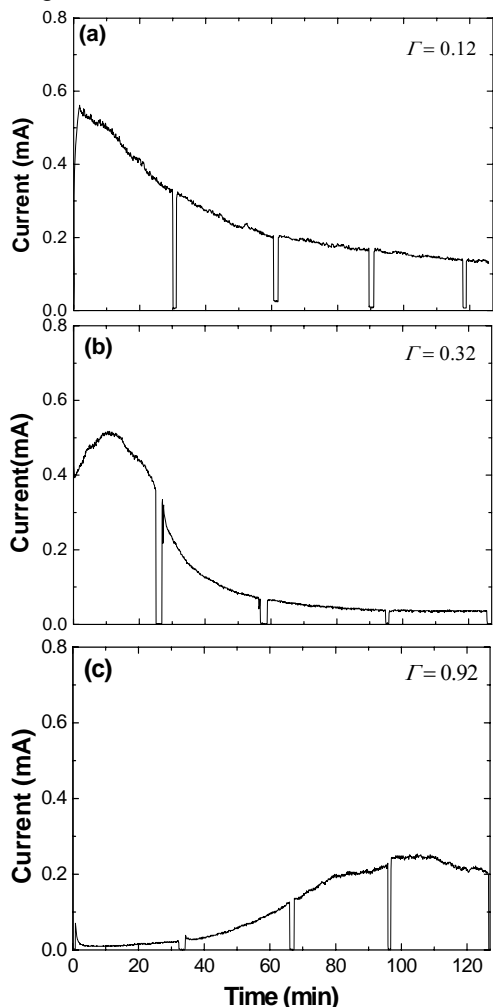
which cut off the UV irradiation in order to allow optical probing of the cell contents. It can be seen that photocurrent is higher for ZnO films obtained with  $\Gamma = 0.12$  in the precursor solution as a function of irradiation than for the other films.



**Figure 6.** SEM micrographs of pyrolytic ZnO films prepared with (a) 0, (b) 0.03, (c) 0.06, (d) 0.12, (e) 0.18, (f) 0.32, and (g) 0.92 ethanol/water molar ratio,  $\Gamma$ , in the precursor solution.

Fig. 8 displays the typical absorbance spectra of the methyl orange solution taken after intervals of 30 - 35 min of photo-electrocatalysis with ZnO films obtained with  $\Gamma$  equal to 0.12, 0.32 and 0.92 in the precursor solution under the UV irradiation. A typical optical absorption peak of methyl orange (17) can be identified at 460 nm. The absorption band of the methyl orange solution drops monotonically after photo-electrocatalysis with ZnO films obtained with  $\Gamma = 0.12$  (Fig. 8a) as a function of the irradiation time, however for ZnO films obtained with  $\Gamma$  equal to 0.32 (Fig. 8b) and 0.92 (Fig. 8c) these absorption bands

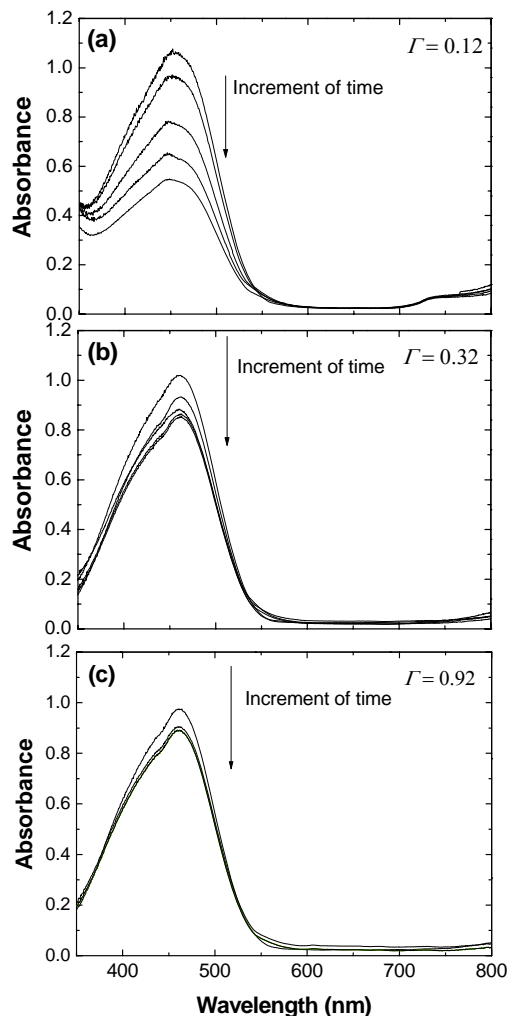
present slight variation, i.e. less photocatalytic degradation of the methyl orange.



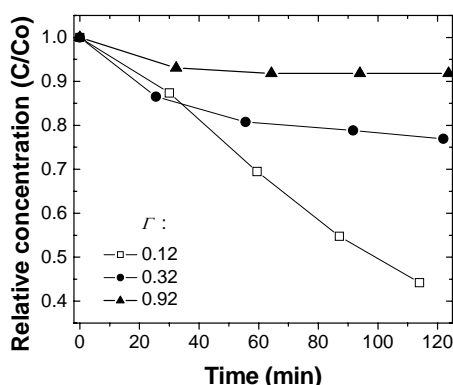
**Figure 7.** Photocurrent as a function of time for UV irradiated pyrolytic ZnO films prepared with (a) 0.12, (b) 0.32, and (c) 0.92 ethanol/water molar ratio,  $\Gamma$ , in the precursor solution in a  $35 \times 10^{-5}$  M of methyl orange water solution.

Figure 9 shows the relative concentration of the methyl orange as a function of the irradiation time using ZnO films obtained with  $\Gamma$  equal to 0.12, 0.32 and 0.92 in the precursor solution. It is shown that the best photodegradation of methyl orange in the solution occurs using ZnO films obtained with  $\Gamma$  equal to 0.12.

From those results there is clear evidence that ZnO induces photo-electrocatalysis degradation of methyl orange, and the degradation rate is related to the film morphology.



**Figure 8.** Spectral absorbance measured after 25 min intervals of UV irradiation for  $35 \times 10^{-5}$  M of methyl orange and pyrolytic ZnO films prepared with (a) 0.12, (b) 0.32, and (c) 0.92 ethanol/water molar ratio,  $\Gamma$ , in the precursor solution.



**Figure 9.** Methyl orange relative concentration as a function of the UV irradiation time for pyrolytic ZnO films prepared with (a) 0.12, (b) 0.32, and (c) 0.92 ethanol/water molar ratio,  $\Gamma$ , in the precursor solution. The initial methyl orange concentration was  $35 \times 10^{-5}$  M.

## 4. Discussion

In-situ measurements of ZnO films growth based on the interference pattern obtained during film deposition were used to monitor the film roughness; it was found that this is related with those results of surfaces and optical analysis obtained by SEM and spectrophotometric measurements, respectively. Those results indicated that there is a correlation between the ethanol/water molar ratio in the spraying solution and the morphology of the obtained ZnO films. The X-ray diffraction patterns revealed that the grain size of the obtained ZnO films is correlated with the ethanol/water molar ratio in the precursor solution. Since we have kept constant the deposition temperature, pH, and concentration of the precursor solution the physical properties of the films are related only to the ethanol/water molar ratio in the spraying solution.

In general, the partial molar volume of a substance A in a mixture is the change in volume on the addition of 1 mol A to a large excess of the mixture (18). The partial molar volumes of the components of a binary mixture of A and B vary with composition because the environment of each type of molecule changes as the composition changes from pure A to pure B. Particularly, the partial molar volume of ethanol in binary mixture of ethanol and water across the full composition has a minimum at ethanol/water molar ratio,  $\Gamma$ , equal to around 0.07. Our results conciliated with the fact that the film roughness and the grain size has a minimum at ethanol/water molar ratio,  $\Gamma$ , equal to 0.06 and 0.12, respectively. The partial molar volumes of ethanol near the minimum are related to higher molecular hydrogen-bridge bounds, which will contribute to enhance the surface tension values of the precursor solution and produce small drops. This can be explained considering that when a molecule of ethanol is added to a huge volume of water, the ethanol molecule is completely surrounded by water molecules and due to their strong hydrogen-bridge bound it is compressed (18). Additional ethanol molecules develops a new hydrogen-bridge bounds between them, which are added to the ones from the water, decreasing even more the partial molar volume of ethanol. However, if the amount of ethanol molecules increases, the hydrogen bridge bounds between the water molecules will decrease and disappear, increasing progressively the partial molar volume of ethanol and the H<sub>2</sub>O molecules will be

surrounded just by ethanol molecules. The hydrogen bridge linkages are responsible for the surface tension values in the solution, and solution with higher surface tension produces larger drops, i.e.: ethanol (surface tension of 24.05 erg/cm<sup>2</sup>) will form smaller drops than water (surface tension of 72.77 erg/cm<sup>2</sup>). Then, a larger amount of sprayed small drops of solution arriving onto the hot substrate will pyrolytically react and spread out onto a larger area than the ones produced from a precursor solution with low surface tension. For  $\Gamma$  lower than 0.06, the partial molar volume of ethanol increases and produces larger drops. These could explain the morphology and grain size of the films.

Films prepared at lower partial molar volume of ethanol respect to water in the spraying solution ( $\Gamma=0.06$  and  $\Gamma=0.03$ ) shown to be mechanically instable in water due that these films are very rough. Films deposited with  $\Gamma\sim 0.06$  in the precursor solution have shown to be the roughest, but the films have a mechanically instability in water. A film obtained with  $\Gamma=0.12$  is still quite rough but mechanically stable in water. In the dark the films prepared with  $\Gamma$  equal to 0.12, 0.32 and 0.92 have good chemical stability, however under illumination the roughest films ( $\Gamma=0.12$ ) decrease its efficiency, this could be due to photocorrosion of the electrode, these fact is also observe to the other films. It has been shown that the ZnO film obtained with  $\Gamma=0.12$  has a noticeable good photoactivity, and after 2 h of UV irradiation the methyl orange degraded to half of the initial concentration. The films obtained with  $\Gamma$  larger than 0.12 or equal to 0.0 are less rough and have small photoactivity. It can be seen that photocurrent (Fig. 7) is higher for rougher film ( $\Gamma=0.12$ ) than for the specular ones, but decreasing in time probably due to i) the diffusion limited rate of dye from the bulk to the interface, ii) photocorrosion of the electrode, or iii) surface poisoning by irreversible adsorption of by products. However, the photocurrent for ZnO film made with  $\Gamma=0.92$  increase with the time, this could be due the photocorrosion of the electrode increments the superficial area. Photo-electrocatalytic results indicated that there is a correlation of the partial molar volume of ethanol respect to water in the spraying solution with the photocatalytic efficiency of the ZnO films.

## 5. Conclusions

Different morphologies of zinc oxide films were obtained when zinc acetate were diluted in different ethanol to water molar ratio,  $L$ , of the precursor solution. We found that the maximum photodegradation of methyl orange in the solution occurs using ZnO films obtained with  $L$  equal to 0.12.

## Acknowledgments

This work was partially supported by SOLWATER project ICA4-CT-2002-10001, ASO Project AE 141/2001 and the International Science Programme of the Uppsala University. Dr. A. Gorenstein is thanked for spectrophotometric measurements at UNICAMP and Dr. J. Santiago for fruitful discussions.

## References

1. Ollis, D. and H. Al-Elkabi, (1993) *Photocatalytic Purification and Treatment of Water and Air*, Elsevier, Amsterdam, Holland.
2. Fujishima, A., K. Hasimoto and T. Watanabe, (1999) *TiO<sub>2</sub> photocatalysis, fundamentals and applications*, BKC, Tokyo, Japan.
3. Domenech, X. and J. Peral, (1999) Kinetics of the photocatalytic oxidation of N(III) and S(IV) on different semiconductor oxides, *Chemosphere* **38**, 1265-1271.
4. Pal, B. and M. Sharon, (2002) Enhanced photocatalytic activity of highly porous ZnO thin films prepared by sol-gel process, *Mater. Chem. Phys.* **76**, 82-87.
5. Jin, M. and L. Shu-Ying, (1994) Preparation of ZnO films by reactive evaporation, *Thin Solid Films* **237**, 16-18.
6. Krzesinsky, A., (1986) A study of the effect of technological parameters of r.f. sputtering on the size of grains and the texture of thin ZnO films, *Thin Solid Films* **138**, 111-120.
7. Ristov, M., Gj. Sinadinovski, I. Grozdanov and M. Mitreski, (1987) Chemical deposition of ZnO films, *Thin Solid Films* **149**, 65-71.
8. Tomar, M. S. and F. J. Garcia, (1982) A ZnO/p-CuInSe<sub>2</sub> thin film solar cell prepared entirely by spray pyrolysis, *Thin Solid Films* **90**, 419-423.
9. Cossement, D. and J. -M. Streydio, (1985) Fabrication of ZnO polycrystalline layers by chemical spray, *J. Cryst. Growth* **72**, 57-60.
10. Fahrenbruch, A. L. and R. H. Bube, (1986) Properties of ZnO films deposited onto InP by spray pyrolysis, *Thin Solid Films* **136**, 1-10.
11. Major, S., A. Banerjee and K. L. Chopra, (1985) Optical and electronic properties of zinc oxide films prepared by spray pyrolysis, *Thin Solid Films* **125**, 179-185.
12. Miki-Yoshida, M., V. Collings-Martinez, P. Amézaga-Madrid and A. Aguilar-Elguézabal, (2002) Thin films of photocatalytic TiO<sub>2</sub> and ZnO deposited inside a tubing by spray pyrolysis, *Thin Solid Films* **419**, 60-64.
13. Miki-Yoshida, M., F. Paraguay-Delgado, W. Estrada-Lopez and E. Andrade, (1999) Structure and morphology of high quality indium-doped ZnO films obtained by spray pyrolysis, *Thin Solid Films* **376**, 99-109.
14. Quintana, M., E. Ricra, J. Rodríguez and W. Estrada, (2002) Spray pyrolysis deposited zinc oxide films for photo-electrocatalytic degradation of methyl orange: influence of the Ph, *Catal. Today* **76**, 141-148.
15. Paraguay D., F., W. Estrada L. D.R. Acosta N., E. Andrade and M. Miki-Yoshida, (2000) Growth, structure and optical characterization of high quality ZnO thin films obtained by spray pyrolysis, *Thin Solid Films* **350**, 192-202.
16. Rodríguez, J., M. Gómez, S.-E. Lindquist and C.G. Granqvist, (2000) Photo-electrocatalytic degradation of 4-chlorophenol over sputter deposited Ti oxide films, *Thin Solid Films* **360**, 250-255.
17. Mills, A. and G. Williams, (1987) Methyl orange as a probe of the semiconductor-electrolyte interfaces in CdS suspensions, *J. Chem. Soc., Faraday Trans. 1*: **83**, 2647-2661.
18. Atkins, P.W., (1994) *Physical Chemistry*, Oxford University Press, Oxford, UK.